Observation and analysis of pellet material ∇B drift on MAST

L. Garzotti[1], K. B. Axon[1], L. Baylor[2], J. Dowling[1], C. Gurl[1], F. Köchl[3], G. P. Maddison[1], H. Nehme[4], A. Patel[1], B. Pégourié[4], M. Price[1], R. Scannell[1], M. Valovič[1], M. Walsh[1]

[1]*Euratom/UKAEA Fusion Association, Culham Science Centre, Abingdon, Oxon, UK*
[2]*Association EURATOM-Österreichische Akademie der Wissenschaften, Austria*
[3]*Oak Ridge National Laboratory, Oak Ridge, Tennessee, USA*
[4]*Association EURATOM-CEA, CEA Cadarache, Saint Paul-lez-Durance, France*

Introduction

Pellet material deposited in a tokamak plasma experiences a drift towards the low field side of the torus induced by the magnetic field gradient. Although difficult to observe, because of the fast time scale on which it occurs and the presence of other transport mechanisms, this ∇B-induced drift has been detected in the past on different machines (ASDEX-U, JET, DIII-D, Tore-Supra, FTU and MAST). Since the fuelling of ITER plasma will rely on the beneficial effect of this ∇B drift to increase the pellet material deposition depth, it is crucial to analyse this phenomenon in detail, develop codes to predict it and compare the predictions with experimental results in present machines.

This paper presents a detailed analysis of this phenomenon based on the unique diagnostic capabilities available on MAST and compares the observations with predictions of state of the art ablation/deposition codes.

Experimental set-up

On MAST deuterium pellets are injected vertically from the top of the machine into the high field side of the plasma. Pellet speed and mass are measured with optical barriers and microwave cavities respectively. Visual analysis of the pellet trajectory and comparison of the pre and post-pellet plasma volume average density are also used to determine the pellet speed and mass. Nominal pellet masses are 0.6, 1.2 and $2.4\cdot10^{20}$ atoms. However, due to losses in the injection track, effective pellet masses can be up to 30% smaller than the nominal ones. Typical pellet speeds are between 250 and 400 m/s.

Typical MAST target plasmas were L-mode and H-mode deuterium plasmas with double null divertor configuration. Main parameters were: plasma current I_p=(0.66-0.76) MA, vacuum toroidal field at the geometric radius B=(0.47-0.50) T, line averaged electron density $\langle n_e \rangle$=$(1.6\text{-}7.5)\cdot10^{19}$ m^{-3} and on-axis electron temperature T_{e0}=(0.7-1.2) keV. H-mode plasmas were NBI heated with launched power P_{NBI}=(1.1-3.0) MW (neutral beam energy 65-67 keV).

Unfiltered visible images of the pellet trajectory inside the plasma were taken with a fast camera with time resolution 5 kfps and exposure time 7 μs. The images allow the analysis of the shape of the pellet cloud and of the pellet trajectory. However, because of the brightness of the pellet cloud, the emitting region around the pellet is saturated and it is not possible to resolve the details of the interior of the cloud. In the future it is foreseen to use an iris to reduce the sensitivity of the camera and analyse the structure of the cloud near the pellet.

A narrow spectrum imaging system [1] with centre wavelength 457 nm and bandpass 2.4 nm, whose field of view included only the final part of the pellet trajectory, recorded the radiation (mainly brehmsstrahlung) emitted by the pellet cloud. The frame rate was 30 fps and the exposure time was 31 ms. The images provided by this second camera saturated on a smaller region of the pellet cloud thus providing, despite the limited view, more detailed information about its structure.

Density and temperature profiles are measured every 5 ms with a multiple-pulse 34 radial points Thomson scattering system and, to analyse the details of the pellet deposition profile, immediately after the end of pellet ablation with a single-pulse 300 radial points Thomson scattering system triggered at the pellet injection time.

Visual and interpretive analysis

A typical image of the trajectory of a pellet injected into a MAST plasma is shown in figure 1. The image is composed by the superposition of 13 frames taken during the pellet ablation at intervals of 200 μs. Images of the pellet cloud taken at different times during the ablation appear as partially overlapping blobs along the pellet trajectory. The image shows also the plasma cross section at the toroidal location of the pellet injection plane, highlighting the flux surfaces from ψ_N=0.1 to ψ_N=1 and spaced by intervals of $\Delta\psi_N$=0.1. The surface highlighted in red corresponds to ψ_N=0.4 and it is the innermost surface affected by the pellet density perturbation according to the Thomson scattering measurement. To enable the estimate of distances on the picture, a square grid lying on the pellet injection plane and spaced by 10 cm is also indicated.

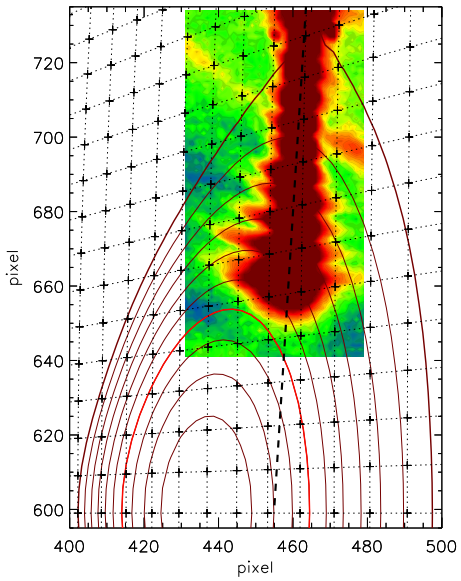

Figure 1. *Composite image of a pellet injected into MAST plasma. The flux surface geometry according to EFIT and a reference grid mapped onto the pellet injection plane are also shown together with a line indicating the pellet trajectory.*

Assuming that the pellet position corresponds to the centre of the light emitting cloud surrounding the pellet itself, analysis of the trajectory shows that the end of the pellet path is located 50 cm above the plasma equatorial plane. In terms of flux surfaces, it can be seen that pellet ablates completely outside ψ_N=0.5-0.6. Therefore to affect the surface ψ_N=0.4 the pellet material should drift by ~20 cm towards the low field side (LFS) of the plasma.

Further, although more questionable, indication of a drift of the pellet material can be obtained from the analysis of the shape of the pellet clouds. From the picture it can be seen that, with respect to the centres of the clouds, which trace out the pellet trajectory, the LFS edge of the clouds seems to extend more significantly towards the LFS of the plasma than the high field side (HFS) edge towards the HFS of the plasma. This asymmetry, which is more evident at the end of the pellet trajectory, suggests that a drift is taking place towards the LFS of the plasma in the direction of the magnetic field gradient. The same asymmetric structure of the pellet cloud is visible on the images taken with the filtered camera.

Finally, it is worth noting that the clouds are equally spaced vertically along the pellet path and the pellet path itself follows, with good approximation, a straight line. These observation exclude the existence of a significant pellet acceleration, induced by rocket effect, along the pellet trajectory. They also seem to exclude a transversal acceleration with respect to the pellet trajectory, although a component of the acceleration directed toward the observer cannot be completely ruled out.

An interpretive analysis of the observation presented above has been performed with the code PELDEP2D [2]. The code calculates the pellet trajectory in the 2-dimensional cross section of the plasma. As the pellet advances along its trajectory, the code calculates the ablation according to the neutral gas and plasma shield (NGPS) ablation model and distributes along the direction of the magnetic field gradient and towards the LFS of the plasma the material ablated at each point of the pellet path. The material is distributed with an exponential shape whose typical length Λ is prescribed and remains the same along the whole trajectory. The particles reaching the plasma edge are recycled with a fuelling efficiency typical of gas puffing (5%). The 2-dimensional density distribution resulting from the

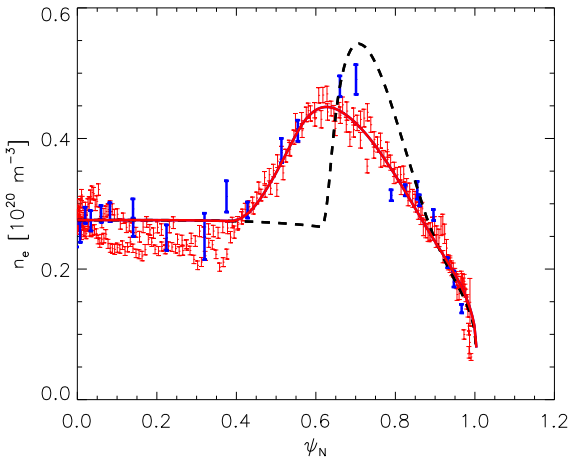

Figure 2. *Ablation and deposition profiles calculated with PELDEP2D compared with Thomson scattering profiles measured at the end of the pellet ablation.*

calculation is averaged over the magnetic surfaces to give a poloidally symmetric deposition profile.

The results of the calculations for the pellet shown in figure 1 are presented in figure 2. The experimental density profile is measured 1 ms after the last frame included in figure 1, which corresponds to the end of the pellet ablation. The red points are the measurements of the high-resolution single-pulse Thompson scattering and the blue points are the measurements of the multi-pulse system. The profiles are mapped on the ψ_N radial co-ordinate and the inner and outer profiles are folded onto each other, showing that a poloidally symmetrical distribution of the ablated material is achieved already immediately at the end of the pellet ablation, which, in this case, lasts ~2.5 ms.

The black dashed line shows the pellet ablation profile calculated without taking into account any drift, whereas the red solid line is the deposition profile calculated including the ∇B drift. It is seen that, while the post-pellet ablation profile calculated taking into account only the pellet ablation falls well outside the experimental data, the drifted profile fits extremely well the experimental measurements. It is worth nothing that the quality of the fit shows a well defined optimum in correspondence of Λ=25 cm, allowing a rather precise estimate of the drift length. It is also interesting to observe how in this case, due to the geometry of the injection, a drift along the magnetic field gradient of the order of 35-40% of the plasma minor radius leads to a displacement of the pellet deposition profile with respect to the ablation profile of only 10-20% in terms of flux radial co-ordinate.

A further question that can be addressed with PELDEP2D is the effect of the plasma pre-cooling, due to the drift of the pellet material in front of the pellet, on the pellet ablation rate and penetration. At every time step PELDEP2D can adiabatically perturb the plasma density and temperature profiles and calculate the pellet ablation using either the perturbed or the unperturbed profiles. Taking into account the cooling effect reduces the ablation rate and gives deeper pellet penetration. It turns out that without pre-cooling the pellet penetrates to 60 cm above the plasma equatorial plane, which is shorter than the observed penetration, whereas when the pre-cooling is taken into account the penetration reaches 50 cm above the equatorial plane, which is closer to the experimental observations. It seems therefore that in MAST the plasma pre-cooling plays a role in reducing the pellet ablation rate and simultaneously increasing the pellet penetration.

Simulations and code predictions

Two predictive codes (developed by Pégourié and co-workers [3] and Parks and co-workers [4] respectively) have been used to predict the drift which should be expected on MAST.

The results of the code described in [3] are shown in figure 3, where the colour code has the same meaning as in figure 2. It can be seen that the predictions of the code are in good agreement with all the results obtained from the interpretive analysis. In particular a displacement between the peak of the ablation and the deposition profile of 0.1 in terms of ψ_N is found and the drift induced plasma pre-cooling had to be taken into account in order to simulate the observed pellet penetration depth. The average drift length of the centre of the plasmoid is of the order of 10 cm. However, since in the predictive code [3] the characteristic

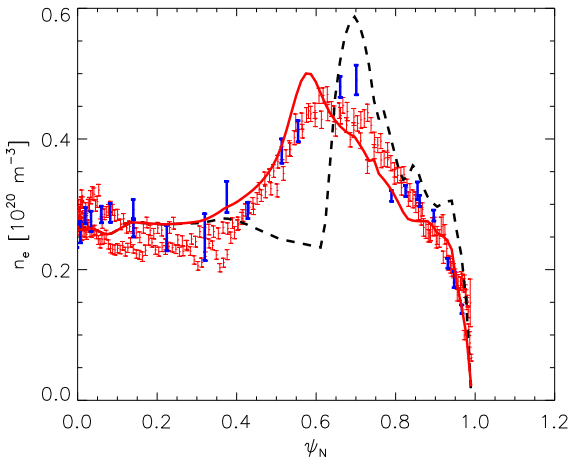

Figure 3. *Ablation and deposition profiles calculated with the predictive code described in [3] compared with Thomson scattering profiles measured at the end of the pellet ablation.*

drift length of the plasmoid varies along the pellet path and the distribution of the ablated material along the ∇B direction has a more realistic shape than a simple exponential one, it is not possible to directly compare this parameter with the adjustable parameter Λ used in PELDEP2D. Indeed, one should compare the poloidally symmetric deposition profiles resulting from the drift and regard the constant drift length Λ used in the interpretive analysis as a simple schematic description of the more realistic plasmoid drift calculated by the predictive code.

The code described in [4] predicts less than half of the drift predicted by the code described in [3]. This is because in this model the drive, which is strongly dependent on the reheating of the pellet cloudlet, requires temperatures over 1 keV to build enough pressure in the cloudlet to accelerate it along the major radius and therefore it is predicted to be weak in MAST, where temperatures are less than 1 keV in the outer part of the plasma where the ablation occurs.

Conclusions

Fast visible imaging and high space and time resolution Thomson scattering revealing the details of the pellet trajectory, ablation and deposition profile on MAST have permitted to identify the existence of a ∇B-induced drift affecting the pellet ablated material. Interpretive analysis of the experimental data show that the drift results in a displacement of 0.1 in terms of ψ_N between the ablation and the deposition profile and that the plasma pre-cooling due to the drift plays a role in determining the pellet penetration depth.

Two advanced first principles ablation/deposition codes have been used to simulate the experimental results. One of them predicts all the observed characteristics of the pellet injection, including the effect of the plasma pre-cooling on the pellet penetration depth, whereas the other tends to underestimate the drift because the driving mechanism is predicted to be weak on MAST. The reason for the discrepancy is probably the different way the two codes describe the dynamics of the plasmoid and further analysis is required to fully understand the differences between the two models and the way they affect the plasmoid drift.

In the future it would be interesting to complement the contribution of MAST data to the characterisation of the ∇B drift phenomenon and to the benchmarking of ablation/deposition codes with similar studies performed on different machines in order to build a more consistent picture in view of the extrapolation of the results to ITER.

Acknowledgments

This work was funded jointly by the United Kingdom Engineering and Physical Sciences Research Council and by the European Communities under the contract of Association between EURATOM and UKAEA. The views and opinions expressed herein do not necessarily reflect those of the European Commission.

References

[1] A. Patel et al., *Rev. Sci. Instrum.* **75** 4944
[2] B. Pégourié and L. Garzotti, *Proc. 24th EPS Conf. on Controlled Fusion and Plasma Physics (Bertchesgaden, 1997)* **21A** 153
[3] B. Pégourié et al., *Nucl. Fusion* **47** 44
[4] P.B. Parks and L.R. Baylor, *Phys Rev. Lett.* **94** 125002